Materialia 14 (2020) 100879

Contents lists available at ScienceDirect

Materialia

journal homepage: www.elsevier.com/locate/mtla

Full Length Article

Nanoparticulation of hyaluronic acid: A new skin penetration enhancing polyion complex formulation: Mechanism and future potential

Miki Shigefuji, Yoshihiro Tokudome*

Laboratory of Dermatological Physiology, Faculty of Pharmacy and Pharmaceutical Sciences, Josai University, 1-1, Keyakidai, Sakado, Saitama 350-0295, Japan

ARTICLE INFO

Keywords:
Skin penetration pathway
Hyaluronic acid
Nanoparticle
Polyion complex
Skin penetration-enhancing technology

ABSTRACT

Skin administration is a simple method of therapeutic and cosmetic application. However, the protective barrier provided by the skin makes it challenging to achieve delivery of high molecular weight compounds. Efforts to improve the penetration of hyaluronic acid (HA) have yielded nanoparticulate polyion complexes of HA with poly-L-lysine (HANP), which act as vehicles for delivering HA deeper into the skin. However, the mechanism for this effect and the response of HANP to the skin environment have not been explored. In this study, the penetration of HANP in skin is compared with that of HA, and differences in the pathways are identified. In addition, the properties of the particles in a simulated skin environment are assessed and HANP are found to show morphological changes in response to ions. These findings are expected to pave the way for future transdermal delivery of other high molecular weight ionic compounds such as proteins.

1. Introduction

The permeation of compounds through the skin is an important route of administration as the application is easy and first pass effects in the liver are avoided. However, the stratum corneum, the outermost layer of the skin, provides a barrier to the penetration of compounds or active cosmetic ingredients that is the regarded as the most significant obstacle to transdermal penetration. Generally, compounds or active cosmetic ingredients that can permeate or penetrate the skin by passive diffusion have a molecular weight of 500 Da or less and are lipophilic [1,2]. Many researchers are currently investigating methods to enhance transdermal absorption and improve the penetration of compounds with low skin permeability. Skin permeation enhancement methods for compounds can be categorized as either physical or chemical enhancement methods. Chemical percutaneous absorption enhancement is applied to relatively low molecular weight compounds. Ethanol and ℓ-menthol have been reported as chemical transdermal absorption enhancers [3,4]. In addition, chemical percutaneous absorption enhancement techniques using ionic liquids, adhesive patches, and gauze patches have been reported [5,6]. These approaches alter the structure of the stratum corneum and reduce its skin barrier function. Physical percutaneous absorption enhancement technology may be used for high molecular weight compounds. Typical examples include microneedles [7], iontophoresis [8], and electroporation [9]. However, these methods have the disadvantage of damaging the skin and being less convenient owing to special equipment being required. In recent years, solid in oil (S/O) technology has been reported in which a water-soluble drug is nano-coated and dispersed in an oily base material to non-invasively penetrate high molecular weight polymer compounds such as insulin or phycocyanin into the skin [10,11]. However, preparations of S/O nano-dispersion require freeze-drying at the preparation stage, which can inactivate the drug [12]. Therefore, S/O technology has not been sufficiently investigated for the delivery of high molecular weight compounds as active substances to the skin by passive diffusion. In addition, it has recently been reported that O/W emulsions can deliver collagen and hyaluronic acid to the skin [13]. However, the skin penetration mechanism has not been reported in detail.

In this study, we focused on polyion complexes (PIC), which are easy to prepare and can form nanoparticles without the use of organic solvents or surfactants. PIC are aggregates formed by cancelling charges as a result of strong electrostatic interactions between oppositely charged polyelectrolytes [14,15]. Generally, since biological components are used, safe nanoparticles can be prepared. In addition, compounds dissolved in water are used without further processing, therefore there is no need to consider denaturing due to temperature. It has been reported that PIC prepared from insulin and chitosan enhance the intestinal absorption of insulin, and calcitonin-loaded spermine PIC and polyacrylic acid PIC improve the oral absorption of calcitonin [16,17]. Thus, PIC have potential as a drug delivery system.

In previous studies, we have reported that the use of hyaluronic acid nanoparticles (HANP) using HA as an anionic compound improved the skin permeability of HA by passive diffusion [18]. HA is a water-soluble high molecular weight polymer that is generally considered to be unable to penetrate the skin by passive diffusion. HANP are expected to

* Corresponding author.

https://doi.org/10.1016/j.mtla.2020.100879
Received 24 June 2020; Accepted 20 August 2020
Available online 22 August 2020

facilitate the deeper penetration of HA into the skin to improve skin properties such as wrinkles and sagging. However, the skin penetration mechanism of HANP and the shape change of particles have not yet been investigated. In this study, HANP were prepared using HA as the anionic compound and poly-L-lysine hydrochloride (PLL) as the cationic compound. In this paper, we aimed to clarify the skin permeation mechanism and particle morphological changes of HANP.

2. Materials and methods

2.1. Materials

Sodium HA (FCH-120, MW 1200 kDa, Purity: 99.9%) was obtained from Kikkoman Biochemifa Company (Tokyo, Japan). PLL, acetaldehyde, cyclohexyl isocyanide, cholesterol, palmitic acid, and sodium cholesteryl sulfate were purchased from Sigma-Aldrich (St. Louis, MO, USA).

5-Aminofluorescein and keratin from wool were purchased from Tokyo Chemical Industry (Tokyo, Japan). Dimethyl sulfoxide, methanol, ethanol, sodium chloride, ammonium acetate, and chloroform were purchased from Fujifilm Wako Pure Chemical Corporation (Osaka, Japan). Ceramide TIC-001 was obtained from Takasago International Corporation (Tokyo, Japan). PBS (phosphate buffered saline) tablets were purchased from Takara Bio (Kusatsu, Shiga, Japan).

2.2. Preparation of fluorescently-labelled HA

Fluorescently-labelled HA (FL-HA) was prepared using a four-component condensation reaction of aldehyde, amine, isocyanide, and carboxylic acid [19], according to a previously reported method [18].

2.3. Preparation of hyaluronic acid nanoparticles

FL-HA aqueous solution (1 mM) and PLL aqueous solution (0.1 mM) were mixed FL-HA: PLL = 1: 2 and stirred at room temperature for 15 min to obtain FL-HANP. HA aqueous solution (0.1 mM) and PLL aqueous solution (0.1 mM) were mixed HA: PLL = 1: 1 and stirred at room temperature for 15 min to obtain HANP. The particle size and polydispersity index (PDI) of the nanoparticles were measured by dynamic light scattering, and the zeta potential was measured by laser doppler electrophoresis using a zetasizer nano ZS (ZEN3600, Malvern Instruments, Malvern, Worcestershire, UK).

2.4. In vitro *skin penetration experiment*

All animal procedures were approved by the Ethics Committee of Josai University (Sakado, Saitama, Japan) in accordance with the National Institute of Health (Tokyo, Japan) (approval number: JU18094 and JU19069).

6-week-old male hairless mice (HOS: HR-1 stain) were purchased from Hoshino Laboratory Animals, Inc. (Bando, Ibaraki, Japan). Full-thickness or stripped skin was mounted in a modified Franz-type diffusion cell with an effective diffusion area of 1.77 cm^2. Test solutions (1.0 mL) were placed on the donor side of the skin. The receiver solution was 5.0 mL of distilled water, which was maintained at 32 °C. Frozen sections of skin were made 24 h after applying the donor solution. The fluorescence in the cross-sectional structure of the skin was observed with a fluorescence microscope (BZ-X710, Keyence, Osaka, Japan). In addition, the stratum corneum was peeled off the full-thickness skin, and the surface of the stratum corneum was observed with a microscope (FV1000D, Olympus, Tokyo, Japan).

2.5. Adsorption of HANP on phospholipid liposomes, keratin, or SC lipid liposomes

Dipalmitoyl phosphatidylcholine (DPPC, Nippon Fine Chemical, Osaka, Japan) was dissolved in chloroform and the solvent was removed under reduced pressure using a rotary evaporator to prepare a lipid film. After the lipid film was hydrated with purified water, freeze-thawing was repeated 5 times. The liposomes were centrifuged at 289,000 × *g* at 4 °C for 15 min (himac CS120GXII, Koki Holdings Co., Ltd. Tokyo, Japan). The obtained precipitate was added to 1 mL of purified water and resuspended to obtain phospholipid liposomes. The phospholipid liposomes and HA aqueous solution or HANP aqueous solution were mixed at a ratio of 1:19 and stirred for 24 h. After centrifugation at 289,000 × *g*, 4 °C for 15 min, the HA in the supernatant was quantified by HPLC. Keratin powder (0.534 mg) and 1 mL of HA or HANP aqueous solution were mixed and stirred for 24 h. After filtration through a 0.45 μm filter (Milex KK, Millipore, MA, USA), the HA in the filtrate was quantified. SCLL were prepared and investigated in the same manner as phospholipid liposomes. The lipid used in the preparation of SCLL was ceramide: cholesterol: palmitic acid, cholesterol sulfate, 40: 25: 25: 10 by wt%. After centrifugation at 289,000 × *g*, 4 °C for 15 min, the HA in the supernatant was quantified by HPLC.

2.6. Quantification of fluorescent HA by HPLC

FL-HA was quantified using a fluorescence HPLC system. The mobile phase was 10 mM ammonium acetate containing methanol (8:2). HPLC separation was performed using a Prominence system (Shimadzu, Kyoto, Japan) with a YMC-Pack Diol-300 column (300 × 8.0 mm, S-5 mm, 30 nm) from YMC CO., LTD. (Kyoto, Japan). The flow rate was 1.0 mL/min. The fluorescence detector (RF-AXL, Shimadzu) was set at excitation: 494 nm, emission: 521 nm.

2.7. Evaluation of lipid fluidity of stratum corneum by attenuated total reflection Fourier transform infrared spectroscopy (ATR-FTIR)

Excised hairless mouse skin was immersed in purified water, 0.05 mM aqueous HA, 0.05 mM aqueous PLL, aqueous HANP, and aqueous FL-HANP for 1, 6, and 24 h. The skin samples were then measured by ATR-FTIR. The measurement conditions were as follows, measurement mode: absorbance, apodization function: Sqr Triangle, integration number: 40 times, resolution: 0.9 cm^{-1}, zero filling: 2 times, temperature: 32 °C. The data sampling range was 600–4000 cm^{-1}.

2.8. Observation of HANP morphology by transmission electron microscopy (TEM)

HANP morphology was observed with a transmission electron microscope (TEM) (JEM-1400 Plus, JEOL Ltd., Tokyo, Japan) using negative staining with a 2% phosphotungstic acid solution. In addition, HANP in PBS solution (final concentration 150 mM) were observed by TEM. The particle size, PDI, and zeta potential of the HANP in both groups were measured using a zetasizer nano ZS.

2.9. Statistical analysis

All data are expressed as the mean ± standard deviation (sd) from at least three independent results. Statistical processing was performed using Student's *t*-test or Dunnett's test by SAS ver 14 (SAS Institute Inc. Campus Drive Cary, NC, USA). Statistical significance level is defined as $p < 0.05$.

3. Results

3.1. Particle preparation

Hyarulonic acid nanoparticles were prepared from HA and PLL. FL-HANP were prepared from FL-HA and PLL.

The particle diameter, PDI, and zeta potential of FL-HANP were 242.5 ± 22.7 nm, 0.58 ± 0.10, and −49.8 ± 3.9 mV, respectively. In contrast, the particle diameter, PDI, and zeta potential of HANP were 92.2 ± 7.8 nm, 0.20 ± 0.03, and −29.5 ± 2.6 mV, respectively (Table 1).

Table 1
Physical properties of HANP and FL-HANP.

Sample	Particle diameter (nm)	PDI	Zeta potential (mV)
FL-HANP	242.5 ± 22.7	0.58±0.10	−49.8 ± 3.9
HANP	92.2 ± 7.8	0.20±0.03	−29.5 ± 2.6

3.2. In vitro *skin penetration study*

The skin penetration of FL-HA and FL-HANP was investigated using stripped hairless mouse skin. In the FL-HA treated group, FL-HA fluorescence was observed on the skin surface. In contrast, in the FL-HANP group, greater penetration of FL-HA into the skin was observed than for non-particle HA (Fig 1a–1h).

Furthermore, when FL-HA or FL-HANP aqueous solution was applied to the full-thickness skin, high fluorescence intensity was observed in the stratum corneum for the FL-HANP application group. The stratum corneum surface was observed by peeling off the stratum corneum. In the FL-HA treated group, fluorescence was observed in the keratinocytes, and in the FL-HANP treated group, fluorescence was observed in the stratum corneum intercellular lipid (Fig. 2a and 2b).

3.3. *Adsorption of HANP on phospholipid liposomes, keratin, or SC lipid liposomes*

The results of the skin penetration study using stripped skin confirmed that treatment with FL-HANP facilitated the penetration of FL-HA deep into the skin. This may be a result of the particle conformation changing the interactions of HA with cell membranes. We confirmed the adsorption of HA and HANP on phospholipid liposomes as an alternative to biological membranes and estimated the interaction between HANP and biological membranes. Phospholipid liposome adsorption of HA and HANP was 4.1% and 35.3%, respectively. That is, the adsorption to phospholipid liposomes was significantly higher for HANP than for HA (Fig. 3a).

In the FL-HA treated group, fluorescence was observed in the keratinocytes, whereas in the FL-HANP treated group, fluorescence was observed in the stratum corneum intercellular lipid. Therefore, we examined the interaction of HANP and HA with keratin and SCLL. The keratin adsorption of HA and HANP was 11.8% and 5.5%, respectively (Fig. 3b). That is, the adsorption to keratin was significantly higher for HA than for HANP. In addition, SCLL adsorption of HA and HANP was 1.2% and 8.2%, respectively. The adsorption to SCLL was significantly higher for HANP than for HA (Fig. 3c).

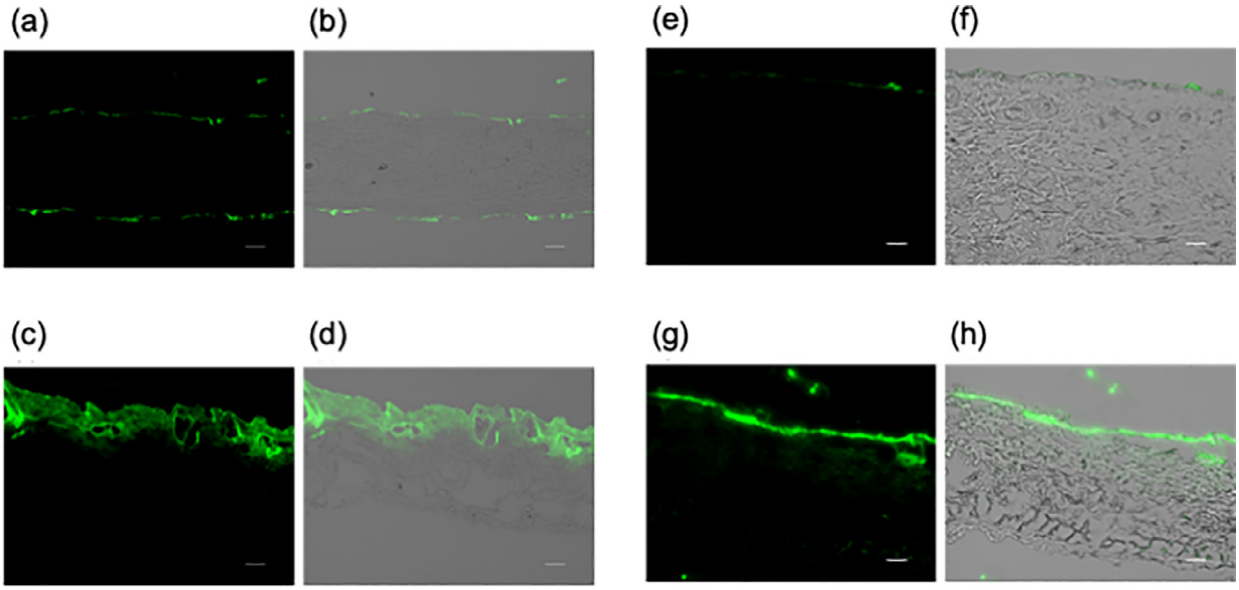

Fig. 1. Cross-sectional fluorescence image of hairless mouse skin. (a) Stripped skin, fluorescence image, HA application, (b) Stripped skin, bright field image, HA application, (c) Stripped skin, fluorescence image, HANP application, (d) Stripped skin, bright field image, HANP application, (e) Full thickness skin, fluorescence image, HA application, (f) Full thickness skin, bright field image, HA application, (g) Full thickness skin, fluorescence image, HANP application, (h) Full thickness skin, bright field image, HANP application. Scale bars indicate 50 μm.

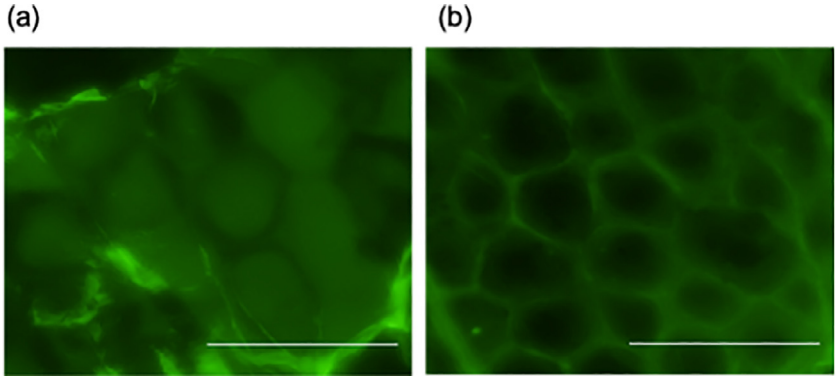

Fig. 2. Skin surface fluorescence image of hairless mouse. (a) Fluorescence image, HA application. (b) Fluorescence image, HANP application. Scale bars indicate 50 μm.

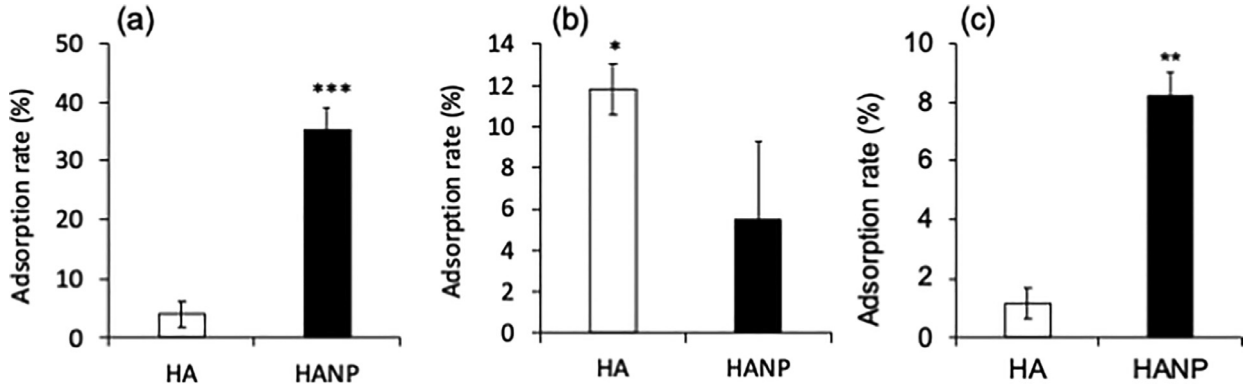

Fig. 3. Adsorption of HANP and HA on (a) phospholipid liposomes, (b) keratin, or (c) SC lipid liposomes. Values represent the mean and standard deviation (SD) of three independent results. Statistical processing was performed using Student's *t*-test. * $p < 0.05$; ** $p < 0.01$; *** $p < 0.001$.

Table 2
Attenuated total reflection Fourier transform infrared spectroscopy (ATR-FTIR) measurements of CH symmetric (a) and asymmetric (b) stretching vibrations in the stratum corneum after 1, 6, and 24 h.

(a)			
	1 h	6 h	24 h
Control	2850.1 ± 0.1	2849.9 ± 0.1	2849.9 ± 0.2
Distilled water	2850.0 ± 0.0	2849.8 ± 0.0	2849.8 ± 0.2
HA	2849.8 ± 0.2	2850.1 ± 0.1	2849.9 ± 0.1
PLL	2849.8 ± 0.0	2849.8 ± 0.1	2849.8 ± 0.0
HANP	2849.9 ± 0.1	2849.9 ± 0.1	2849.8 ± 0.0
FL-HANP	2850.1 ± 0.2	2849.8 ± 0.1	2849.9 ± 0.1
(b)			
	1 h	6 h	24 h
Control	2917.6 ± 0.3	2917.6 ± 0.1	2917.3 ± 0.2
Distilled water	2917.4 ± 0.2	2917.4 ± 0.1	2917.6 ± 0.4
HA	2917.3 ± 0.2	2918.0 ± 0.3	2917.7 ± 0.2
PLL	2917.3 ± 0.2	2917.5 ± 0.0	2917.6 ± 0.1
HANP	2917.3 ± 0.2	2917.5 ± 0.4	2917.8 ± 0.6
FL-HANP	2917.8 ± 0.3	2917.6 ± 0.2	2918.0 ± 0.1

Samples: Control (stratum corneum only), Distilled water (vehicle), HA (hyaluronic acid), PLL (poly L-lysine), HANP (hyaluronic acid nanoparticle), FL-HANP (fluorescently labeled HANP). Values represent the mean and standard deviation (SD) of three independent results.

3.4. Intercellular lipid fluidity of stratum corneum lipid by ATR-FTIR

The CH symmetric stretching vibration shift (around 2850 cm^{-1}) and CH asymmetric stretching vibration shift (around 2920 cm^{-1}) following the application of HA or HANP to mouse skin were measured by ATR-FTIR. No significant peak shift was observed for any of the groups (Table 2).

3.5. TEM observation of HANP

The morphology of the HANP was observed by TEM. The particles were ~150 nm and had heterogeneous hydrophilic and lipophilic domains (Fig. 4a and 4b). In addition, we mixed HANP and PBS (final concentration: 150 mM) to estimate whether the particles would retain their shape when they penetrated the skin. HANP were observed to change shape in the presence of coexisting ions (Fig. 4c and 4d). The physical properties of HANP also changed significantly as a result of the morphological change (Fig. 5a, 5b, and 5c).

4. Discussion

The purpose of this study was to investigate the passive skin penetration of PIC composed of hydrophilic high molecular weight compounds and elucidate their penetration pathway.

It was shown that nanoparticles could be prepared from an aqueous HA or FL-HA solution and an aqueous PLL solution.

First, an *in vitro* skin penetration study was carried out through excised stripped hairless mouse skin. FL-HA stayed in the upper layer of the stripped skin, while FL-HANP delivered HA inside the stripped skin. In general, the penetration of compounds into the skin follows Fick's first and second law. That is, the distribution of the compound from the skin and the diffusion of the compound to the skin are important. Generally, high molecular weight (MW=1200 kDa) and water-soluble compounds as a hyaluronic acid are difficult to diffuse through the skin [1,18]. We found that the diffusivity of the stripped skin was lower for HA and was therefore greatly improved by the nanoparticulation (Fig. 1). In general, the permeability of skin to a compound is proportional to the diffusion coefficient by Fick's first and second laws. Improving diffusion therefore increases skin penetration. Although the details are unknown, HA was able to diffuse easily into skin as a nanoparticulate. Next, an *in vitro* skin penetration study through the full thickness skin of hairless mice was carried out. It was found that HA was only present on the surface of the stratum corneum in the FL-HA treated group, while in contrast, permeation of FL-HA into the stratum corneum was confirmed for the FL-HANP treated group. This result suggests that the skin permeability of water-soluble high molecular weight compounds such as hyaluronic acid, which are generally considered poor at penetrating the skin, can be improved if they adopt a nanoparticle conformation. Following the skin penetration study, the stratum corneum was peeled from the full thickness skin, and the skin surface was observed using a fluorescence microscope. Fluorescence was observed in the keratinocytes for the FL-HA treated group and in the stratum corneum intercellular lipid for the FL-HANP treated group (Fig. 2a and 2b). The percutaneous absorption routes of general compounds are identified as either transcellular or intercellular. Hydrophilic compounds are distributed in the stratum corneum via the transcellular route, and lipophilic compounds are distributed via the intercellular route [20]. Our results indicate that HA penetrates the skin via an transcellular route, while HANP penetrates the skin via an intercellular route. It was therefore strongly suggested that converting HA to nanoparticles altered the penetration pathway.

The route of HA and HANP penetration into the skin was investigated. Since the skin surface from which the stratum corneum was removed was considered a cell membrane of living cells, the adsorptivity to the living cell membrane was examined using phospholipid liposomes. HANP showed significantly higher adsorption than HA to phospholipid liposomes (Fig. 3a). This result shows a similar tendency to that revealed by the section image obtained for the skin penetration test using stripped skin, and supports the higher skin penetration of HANP compared with non-particle HA. This suggests that, compared with HA, HANP enhances skin permeability as a result of stronger interaction with biological membranes.

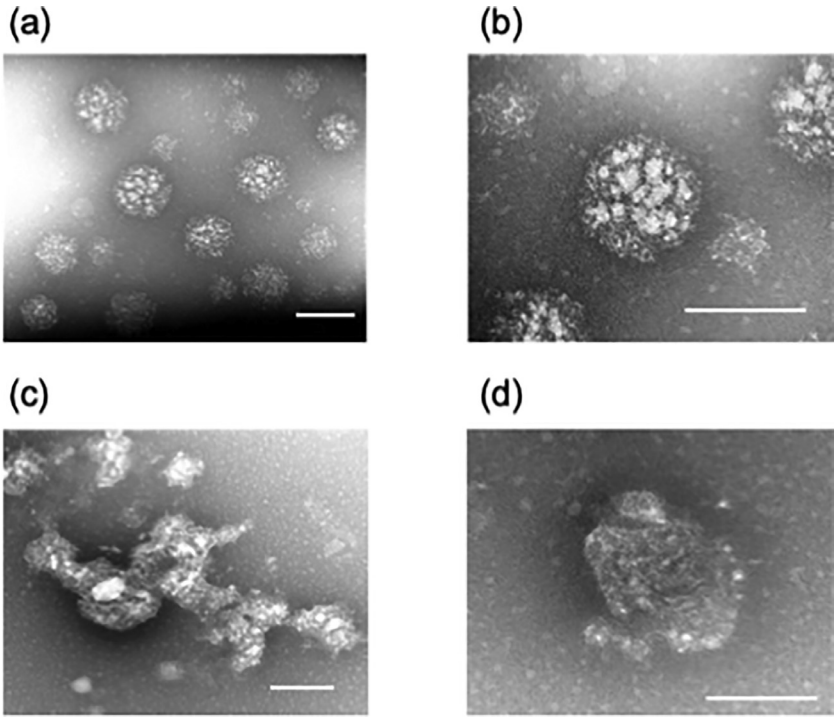

Fig. 4. Observation of HANP morphology by transmission electron microscopy (TEM). (a) HANP and distilled water, (b) HANP and PBS (final concentration: 150 mM), (c) HANP and distilled water (enlarged view), (d) HANP and PBS (final concentration: 150 mM) (enlarged view). Scale bar indicates 200 nm.

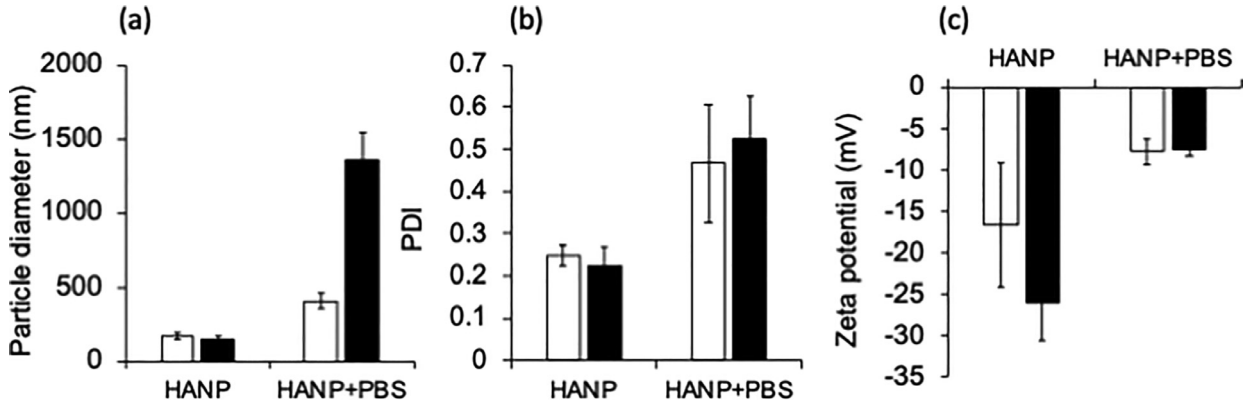

Fig. 5. Particle diameter, PDI, and zeta potential of HANP and HANP on addition of PBS. (final concentration of 150 mM). (a) Particle diameter, (b) PDI, (c) zeta potential. Values represent the mean and standard deviation (SD) of three independent results.

In light of these findings, we concluded that HA and HANP penetrated the stratum corneum via different pathways. We then investigated how HA and HANP interact with keratinocytes and the intracellular lipids of keratinocytes. First, the interaction between keratinocytes and HA or HANP was investigated based on their adsorption to keratin, the main component of keratinocytes. The adsorption of HANP to keratin was significantly lower than that of HA (Fig. 3b).

In addition, the adsorptivity of HA and HANP to SCLL was examined using a similar method. The adsorption of HANP to SCLL was significantly higher than the adsorption of HA to SCLL (Fig. 3c). HA—a water-soluble polymer—has a high adsorptivity to keratinocytes, therefore it does not penetrate deep into the skin and remains on the surface. In contrast it suggests that HANP penetrates the skin via intercellular lipids. The transcellular pathway through keratinocytes requires that the cell membrane is penetrated at least twice [20]. Generally, lipophilic compounds show greater skin permeability than hydrophilic compounds [2]. It may therefore be possible to improve skin penetration if a lipophilic compound penetration pathway (intercellular route) is available. It has been shown that the formation of nanoparticles makes it possible to alter the water-soluble polymer compound so that it penetrates the skin via a route that is more conducive to penetration. These results suggest that after passing through the stratum corneum, HANP is strongly adsorbed to living cell membranes. Thus, it was shown that nanoparticles based on PIC technology could penetrate deeper into the skin after passing through the stratum corneum than non-particulate compounds.

The lipid fluidity of the stratum corneum after application of HANP to the skin was investigated using ATR-FTIR. The peaks around 2850 cm^{-1} and 2920 cm^{-1} that are specifically detected for stratum corneum lipids are attributed to the CH_2 symmetric stretching vibration and CH_2 antisymmetric stretching vibration, respectively [21]. Shifts of these peaks to higher wavenumbers indicate a conformational change from the trans conformation to the gauche conformation [22], and increasing the gauche conformation reduces lipid packing efficiency [23]. Therefore, as lipid fluidity increases, the infrared absorption shifts to higher wavenumbers [24]. No peak shift was observed for any of the HANP, HA, and PLL samples compared with the control group (Table 2). This result indicates that there was no significant change in the fluidity of the intercellular lipids. The improvement of skin permeability to HA resulting from HANP formation was found to result in low breakdown of lipids, it is therefore not expected to have a greater effect

on skin barrier function than conventional penetration enhancement techniques.

Finally, to simulate the morphological change of HANP after application to the skin, the physical properties were measured under the conditions that mimicked the skin surface. The addition of PBS significantly increased the particle size and PDI of HANP (Fig. 5a, 5b, and 5c). In addition, the absolute value of the zeta potential was significantly reduced. A TEM image was also acquired under the same conditions. The addition of PBS to HANP changed the HANP morphology (Fig. 4a, 4c), indicating that coexisting ions cause HANP to aggregate or break down. This was thought to be due to the disruption of the electrostatic interactions within HANP by ions, it was therefore speculated that a similar effect would be observed when HANP were applied to the skin, as a result of reacting with ions in the skin. This suggests that HANP break down after penetrating the skin and then function as HA in the skin. However, it is not clear whether HANP is destroyed on the skin surface when it comes into contact with the stratum corneum, or whether it breaks down on the skin after penetrating the stratum corneum. We previously reported that HANP exist as non-nanoparticulated HA in the skin after application to the skin [18]. As mentioned above, ions are thought to have a significant effect on the breakdown of HANP. It is therefore more likely that higher ionic strength will affect the structure of the nanoparticles. It has been reported that the calcium ion concentration in the stratum corneum is low and the concentration of calcium ions increases in the direction of the dermis. Thus, HANP do not disintegrate shortly after application to the skin, and are expected to disintegrate slowly upon penetration into the skin, however this requires further investigation. In addition, certain factors relating to counter ions such as PLL remain unclear. It is necessary to continue to investigate the localization of the PLL after applying it to the skin as HANP, and the particle formation efficiency.

Contributions

M.S. and Y.T. designed and performed experiments analyzed the data, and wrote first version of manuscript. M.S. and Y.T. performed part of experiments. M.S. and Y.T. designed experiments and supervised the study. Y.T. wrote the manuscript. All authors contributed to the critical revision of the manuscript and approved the final version.

Declaration of Competing Interest

The authors have no conflict of interest to declare.

Acknowledgment

We thank Sarah Dodds, PhD, from Edanz Group (https://en-author-services.edanzgroup.com/) for editing a draft of this manuscript and helping to draft the abstract.

Funding

This work was supported by the KOSÉ Cosmetology Research Foundation: Grant Number 669 to Yoshihiro Tokudome.

References

[1] J.D. Bos, M.M. Meinardi, The 500 Dalton rule for the skin penetration of chemical compounds and drugs, Exp. Dermatol. 9 (2000) 165–169, doi:10.1034/j.1600-0625.2000.009003165.x.

[2] G.L. Flynn, S.H. Yalkowsky, Correlation and prediction of mass transport across membranes I: influence of alkyl chain length on flux-determining properties of barrier and diffusant, J. Pharm. Sci. 61 (1972) 838–852, doi:10.1002/jps.2600610603.

[3] T. Marjukka Suhonen, J.A. Bouwstra, A. Urtti, Chemical enhancement of percutaneous absorption in relation to stratum corneum structural alterations, J. Control. Rel. 59 (1999) 149–161, doi:10.1016/S0168-3659(98)00187-4.

[4] J.R. Kunta, V.R. Goskonda, H.O. Brotherton, M.A. Khan, I.K. Reddy, Effect of menthol and related terpenes on the percutaneous absorption of propranolol across excised hairless mouse skin, J. Pharm. Sci. 86 (1997) 1369–1373, doi:10.1021/js970161.

[5] M. Zakrewsky, K.S. Lovejoy, T.L. Kern, T.E. Miller, V. Le, A. Nagy, et al., Ionic liquids as a class of materials for transdermal delivery and pathogen neutralization, Proc. Natl. Acad. Sci. U.S.A. 111 (2014) 13313–13318, doi:10.1073/pnas.1403995111.

[6] N. Shinkai, K. Korenaga, H. Mizu, H. Yamauchi, Intra-articular penetration of ketoprofen and analgesic effects after topical patch application in rats, J. Control. Rel. 131 (2008) 107–112, doi:10.1016/j.jconrel.2008.07.012.

[7] S. Henry, D.V. McAllister, M.G. Allen, M.R. Prausnitz, Microfabricated microneedles: a novel approach to transdermal drug delivery, J. Pharm. Sci. 87 (1998) 922–925, doi:10.1021/js980042.

[8] L. Langkjær, J. Brange, G.M. Grodsky, R.H. Guy, Iontophoresis of monomeric insulin analogues *in vitro*: effects of insulin charge and skin pretreatment, J. Control. Rel. 51 (1998) 47–56, doi:10.1016/S0168-3659(97)00155-7.

[9] M.R. Prausnitz, V.G. Bose, R. Langer, J.C. Weaver, Electroporation of mammalian skin: a mechanism to enhance transdermal drug delivery, Proc. Natl. Acad. Sci. U.S.A. 90 (1993) 10504–10508, doi:10.1073/pnas.90.22.10504.

[10] Y. Tahara, S. Honda, N. Kamiya, H. Piao, A. Hirata, E. Hayakawa, et al., A solid-in-oil nanodispersion for transcutaneous protein delivery, J. Control. Rel. 131 (2008) 14–18, doi:10.1016/j.jconrel.2008.07.015.

[11] S.D. Hardiningtyas, S. Nagao, E. Yamamoto, N. Shirakigawa, R. Wakabayashi, M. Goto, et al., A nano-sized gel-in-oil suspension for transcutaneous protein delivery, Int. J. Pharm. 567 (2019) 118495, doi:10.1016/j.ijpharm.2019.118495.

[12] M. Kitaoka, R. Wakabayashi, N. Kamiya, M. Goto, Solid-in-oil nanodispersions for transdermal drug delivery systems, Biotechnol. J. 11 (2016) 1375–1385, doi:10.1002/biot.201600081.

[13] P. Szumała, C. Jungnickel, K. Kozłowska-Tylingo, B. Jacyna, K. Calc, Transdermal transport of collagen and hyaluronic acid using water in oil microemulsion, Int. J. Pharm. 572 (2019) 118738.

[14] H. Dautzenberg, Polyelectrolyte complex formation in highly aggregating systems. 1. Effect of salt: polyelectrolyte complex formation in the presence of NaCl, Macromolecules 30 (1997) 7810–7815, doi:10.1021/ma970803f.

[15] C. Schatz, J.-M. Lucas, C. Viton, A. Domard, C. Pichot, T. Delair, Formation and properties of positively charged colloids based on polyelectrolyte complexes of biopolymers, Langmuir 20 (2004) 7766–7778, doi:10.1021/la049460m.

[16] A. Makhlof, M. Werle, Y. Tozuka, H. Takeuchi, A mucoadhesive nanoparticulate system for the simultaneous delivery of macromolecules and permeation enhancers to the intestinal mucosa, J. Control. Rel. 149 (2011) 81–88, doi:10.1016/j.jconrel.2010.02.001.

[17] P. Mukhopadhyay, K. Sarkar, M. Chakraborty, S. Bhattacharya, R. Mishra, P.P. Kundu, Oral insulin delivery by self-assembled chitosan nanoparticles: *in vitro* and *in vivo* studies in diabetic animal model, Mater. Sci. Eng. C Mater. Biol. Appl. 33 (2013) 376–382, doi:10.1016/j.msec.2012.09.001.

[18] Y. Tokudome, T. Komi, A. Omata, M. Sekita, A new strategy for the passive skin delivery of nanoparticulate, high molecular weight hyaluronic acid prepared by a polyion complex method, Sci. Rep. 8 (2018) 2336, doi:10.1038/s41598-018-20805-3.

[19] A.N. de Belder, K.O. Wik, Preparation and properties of fluorescein-labelled hyaluronate, Carbohydr. Res. 44 (1975) 251–257, doi:10.1016/s0008-6215(00)84168-3.

[20] B.W. Barry, Mode of action of penetration enhancers in human skin, J. Control. Rel. 6 (1987) 85–97, doi:10.1016/0168-3659(87)90066-6.

[21] G. Bernard, M. Auger, J. Soucy, R. Pouliot, Physical characterization of the stratum corneum of an *in vitro* psoriatic skin model by ATR-FTIR and Raman spectroscopies, Biochim. Biophys. Acta 1770 (2007) 1317–1323, doi:10.1016/j.bbagen.2007.06.014.

[22] H.K. Vaddi, P.C. Ho, Y.W. Chan, S.Y. Chan, Terpenes in ethanol: haloperidol permeation and partition through human skin and stratum corneum changes, J. Control. Rel. 81 (2002) 121–133, doi:10.1016/S0168-3659(02)00057-3.

[23] T. Marjukka Suhonen, J.A. Bouwstra, A. Urtti, Chemical enhancement of percutaneous absorption in relation to stratum corneum structural alterations, J. Control. Rel. 59 (1999) 149–161, doi:10.1016/S0168-3659(98)00187-4.

[24] R.O. Potts, G.M. Golden, M.L. Francoeur, V.H.W. Mak, R.H. Guy, Mechanism and enhancement of solute transport across the stratum corneum, J. Control. Rel. 15 (1991) 249–260, doi:10.1016/0168-3659(91)90116-U.